Amorphous Microporous Titania Modified with Platinum(IV) Chloride—A New Type of Hybrid Photocatalyst for Visible Light Detoxification

Ling Zang,[†] Christian Lange,[‡] Ingo Abraham,[‡] Sebastian Storck,[‡] Wilhelm F. Maier,*[,‡] and Horst Kisch*[,†]

Institut für Anorganische Chemie der Universität Erlangen-Nürnberg, D-91058 Erlangen, and Max-Planck-Institut für Kohlenforschung, D-45470 Mülheim, Germany

Received: April 7, 1998; In Final Form: August 16, 1998

Amorphous microporous metal oxides of titanium (AMM-Ti) modified with a few percent of a platinum(IV) halide have been prepared by a sol−gel procedure and characterized by various surface analytical methods. By these methods the metal salt is homogeneously distributed in an almost exclusively amorphous powder of high specific surface area (160−200 m^2/g) and a pore size of 0.8 nm. From the coordination number of 4.3 and a Pt−Cl distance of 2.28 Å, as calculated from extended X-ray absorption fine structure results, we conclude that the platinum salt is present as $PtCl_4$. The hybrid sample (Pt(IV)/AMM-Ti) catalyzes the photodegradation of 4-chlorophenol with visible light. Apparent disappearance quantum yields decrease from 8.6×10^{-3} at 335 nm to 4.5×10^{-3} at 366 nm and 2.8×10^{-3} at 400 nm; lower values of 1.6×10^{-3} and 1.3×10^{-3} are found at 436 and 546 nm, respectively. The quantum yield at both 366 and 436 nm decreases linearly with the square root of the incident photon flux, suggesting increasing recombination of the photogenerated charge carriers. We postulate that the photocatalytic activity of Pt(IV)/AMM-Ti originates from local excitation of the platinum(IV) chloride chromophore, affording a halogen atom and Pt(III) as intermediate species. Charge-trapping by the titania matrix generates reducing and oxidizing surface sites from which subsequent photodegradation proceeds. Good photostability of Pt(IV)/AMM-Ti is demonstrated by repeated use of the photocatalyst.

Introduction

Because of its high catalytic activity and photostability, colloidal or powder titania has been widely used as a photocatalyst for light-to-energy conversion[1] and chemical transformations.[2] Particularly from the point of practical application, TiO_2 is a promising photocatalyst for water purification,[3] given that most of the organic contaminants in water can be readily degraded in the presence of oxygen. During the past decades much attention has been paid to the improvement of the photocatalytic activity of TiO_2. One severe disadvantage of this semiconductor material is the large band gap, 3.2 eV for bulk TiO_2, which limits its photosensitivity to the ultraviolet region.

To improve the response of TiO_2 to visible light, various methods have been used. One of the best-investigated methods is dye-sensitization,[4] which has been extensively developed in photoelectrochemical systems. However, these systems cannot be used for detoxification of wastewaters, since the dye molecules will also be consumed in the process. Another method couples TiO_2 with a small−band gap semiconductor (e.g., CdS).[5−8] Upon excitation with visible light, electron-hole pairs are produced in the CdS particle. Because of the difference of band levels between the two semiconductors, the electron is subsequently transferred to the conduction band of TiO_2, while the hole remains in the valence band of CdS, thereby attaining an efficient charge separation. One fatal obstacle of these composite materials is the photoanodic corrosion of the CdS, especially in the presence of oxygen. Chromic ion−doped TiO_2 has been reported to be photoactive for sustained water cleavage in the visible region.[9] Mixed-phase Ti/Fe oxide colloids containing from 0.1 to 50 at. % Fe have also been prepared,[10] in which the mixed oxides show some activity for photocatalytic degradation of dichloroacetate when irradiated with visible light. However, the reaction is accompanied by cathodic dissolution of the ferric oxide, even though this could be eliminated to some extent by addition of oxidants such as H_2O_2. In fact, as discussed in several excellent reviews,[2,11] the detailed mechanism for the metal ion−doped semiconductors remains a controversial issue. Although many studies have reported the improvement of the photocatalytic activity of TiO_2 by doping with transition metal ions, several researchers have found the opposite.

In connection with our previous work on the use of amorphous zinc and cadmium sulfide as photocatalysts for novel chemical syntheses,[12] we report here a new type of amorphous TiO_2 catalyst modified with platinum(IV) chloride, which belongs to the class of amorphous microporous metal oxides (AMM) developed for applications in heterogeneous catalysis.[13] The material preparation is based on a modified sol−gel process, which allows control of the pore size, the surface polarity, and the chemical composition in a single preparation step.[14,15] During the development of this synthesis, special emphasis was paid to the atomic or molecular isolation of the active center in the porous matrix of the bulk material. Such materials have already shown unique properties as shape-selective hydrocracking catalysts,[16] selective solid acids,[17] and selective oxidation and hydrogenation catalysts.[18,19] In the past, noble metal−containing AMM catalysts have always been reduced prior to

* Authors for correspondence.
[†] Universität Erlangen-Nürnberg.
[‡] Max-Planck-Institut.

10.1021/jp981755j CCC: $15.00
Published on Web 12/05/1998

catalytic applications.[20] This use as photocatalyst is therefore the first AMM application in which the noble metals are utilized in their oxidized form. Here we report our investigation of photocatalytic activity using 4-chlorophenol (4-CP) as a probe compound, the photodegradation of which has been extensively studied.[11]

Experimental Section

Materials. 4-CP, hydroquinone (HQ), and all the other agents were of analytical grade and used without further purification. Titanium isopropoxide and $[Ru(bipy)_3]^{2+}$, used as a chemical actinometer, were purchased from Aldrich. The TiO_2 powder (P-25), consisting mainly of anatase, was obtained from Degussa Company. Triply distilled water was used throughout this study.

The hybrid titania (Pt(IV)/AMM-Ti) was prepared by a sol−gel procedure through slow hydrolysis of titanium isopropoxide in the presence of $PtCl_6^{2-}$ ions in a strong acidic aqueous media.[18] As an example, the catalyst containing 1.1% (weight percent) of Pt(IV), usually referred to hereafter as Pt(IV)/AMM-Ti, was prepared as follows: 12 mL of $Ti(OC_3H_7)_4$ (0.04 mol) was dissolved in 50 mL of ethanol and stirred for 30 min, followed by slow addition of 0.1 mL of 8 M HCl acid. After 5 min, 0.1 mL of concentrated HCl was added; after 10 min, 0.3 mL; and after a further 10 min, 0.3 mL. Thereafter, 0.105 g (1.87×10^{-4} mol) of $Na_2PtCl_6 \cdot 6H_2O$ dissolved in 10 mL of ethanol was added slowly. The clear yellow solution obtained was then stirred at room temperature for 1 day. Thereafter, without stirring, the loosely covered sol gelled within 6 days of standing at room temperature. For further mild drying, the gel was kept uncovered for another 10 days in a hood, after which it turned hard and brittle. The solidified gel was heated to 65 °C at a heating rate of 0.1 °C/min, kept at this temperature for 100 min, and then heated at the same rate to 250 °C. After this temperature was sustained for 300 min, cooling to room temperature was allowed at a rate of 0.5 °C/min. Most of the photodegradations in this study were performed with Pt(IV)/AMM-Ti. The unmodified titania (AMM-Ti) was prepared by the same procedure but in the absence of a platinum salt. Before use as a photocatalyst, materials were ground in a ball mill, which provided small particles suitable for suspension in water.

The corresponding bromide-modified sample was obtained by the same method but with use of $PtBr_4$ and HNO_3. Two kinds of TiO_2-PtO_2 mixed oxides were prepared and used for comparative investigations in this study: amorphous TiO_2 bulk-doped with PtO_2, and TiO_2 with surface-deposited PtO_2. The former was prepared by a cohydrolysis method and subsequent coprecipitation. $Ti(OC_3H_7)_4$ (3.46 g) was dissolved in 20 mL of 2-propanol and slowly added, with stirring, to 30 mL of 0.1 M HCl solution containing 26.7 mg of $H_2PtCl_6 \cdot 6H_2O$ (10.7 mg of Pt). After stirring overnight, a light yellow gel was obtained. The gel was adjusted to pH >12.0 by addition of concentrated NaOH solution. The basic gel was dried carefully at 100 °C by air-bubbling. The dark brown powder thus obtained was washed with water five times to remove the excess ions, followed by drying and aging at 60 °C for 1 day. The resulting sample contained 1.3% Pt (assuming all the platinum salts were converted to PtO_2). The TiO_2 with surface-deposited PtO_2 (also 1.3% Pt) was prepared by suspending 50 mg of AMM-Ti in 50 mL of water containing 1.6 mg of $H_2PtCl_6 \cdot 6H_2O$ (0.65 mg of Pt) and stirring overnight. The suspension was then adjusted to pH >12.0 and dried at 100 °C. The brown powder obtained was washed and aged the same way as above.

Apparatus. *(a) Physisorption:* For characterization of the pore structure and determination of the specific surface area of Pt(IV)/AMM-Ti powders, the argon isotherm was measured on a Coulter Omnisorb 360 at 87 K by using a static-flow volumetric method in the pressure range of $p/p_0 = 0-1$. The powder was heated to 523 K for 48 h at 10^{-5} Pa prior to the measurement. The surface area was calculated by using the Brunauer−Emmett−Teller equation in the range of $p/p_0 = 0-0.3$. Micropore size distribution was calculated from the Ar-adsorption isotherm with the Horvath−Kawazoe method for microporous solids.[21]

(b) HRTEM: The distribution of Pt species in the TiO_2 matrix was investigated with high-resolution transmission electron microscopy (HRTEM) on a Hitachi HF 2000 instrument at 200 keV combined with energy-dispersive X-ray analysis (EDX). With the microscope used, the EDX beam can be condensed to a diameter of 1−2 nm, allowing determination of elemental composition with high resolution. The sample was crushed in an agate mortar in a methanol suspension and transferred to a Holey carbon grid (copper, 3 mm diameter).

(c) X-ray Diffraction: Powder X-ray diffraction (XRD) patterns were measured by using the Debye−Scherrer technique on a Stoe Stadi 2/PL diffractometer with Cu K_α radiation in the range of $2\theta = 10-80°$ and the area detector PSD1. The temperature dependence of the patterns was recorded in the range from 293 to 1173 K (increasing stepwise by 50 K prior to each measurement).

(d) Diffuse Reflectance Spectroscopy: Diffuse reflectance spectra of the powders were measured on a Shimadzu UV-3101PC, UV−vis−NIR scanning spectrophotometer equipped with a diffuse reflectance accessory. The samples were spread onto an Al_2O_3 plate, the background reflectance of which had been measured before. The reflectance data were converted by the instrument software to the $F(R_\infty)$ values according to Kubelka−Munk theory.[22]

(e) EXAFS Data Acquisition and Analysis: Extended X-ray absorption fine structure (EXAFS) measurements above the platinum L_{III} absorption edge were performed on the Pt(IV)/AMM-Ti sample mixed with polyethylene. The experiments were carried out at room temperature in transmission geometry at beamline A1 at HASYLAB in Hamburg with a Si(311) double-crystal monochromator. The tilt of the second monochromator crystal was set to 40% harmonic rejection. Three 30-cm-long ionization chambers, flushed successively with nitrogen and argon, were used to record the intensities I_0, I_1, and I_2 of the synchrotron radiation before and behind the samples and behind a platinum foil, which was used to check the energy calibration of the monochromator during the measurements. Above the absorption edge, data were recorded equidistantly in k space, with $\Delta k = 0.04$ Å^{-1}. The sampling time at each data point was increased from 1 s at the beginning of a spectrum to 6 s at its end. The absorption jump $\Delta\mu d$ was 0.07 and five spectra were added. The absorption spectra $\mu(E) = \ln(I_0(E)/I_1(E))$ were analyzed according to the literature.[23] In the first step, background absorption was removed by subtraction of Victoreen-type polynomials. To determine the smooth parts of the background-subtracted spectra, we used a modified smoothing spline algorithm. After division of the background-subtracted spectra by their smooth parts, photon energies E were converted to photoelectron wavenumbers k by using the photoelectron threshold energy E_0 as a free parameter. The resulting $\chi(k)$ functions were multiplied with k^3 and Fourier-filtered, i.e., Fourier-transformed to r space, multiplied with a square window function, and transformed back to k space. The

Fourier-filtering range was 1.0−2.9. Data analysis in *k* space was performed according to the curved-wave single-scattering formalism with theoretical scattering functions, calculated with the program FEFF6[24] for several crystalline platinum compounds. As structural parameters, the absorber backscatterer distance, the coordination number, and the EXAFS Debye−Waller factor were determined for the first coordination shell. The final fits were performed with theoretical scattering functions calculated for crystalline $PtCl_4$ and with $E_0 = 11571$ eV.

Photodegradation Procedure and Product Analysis. The photocatalytic degradation of 4-CP was carried out in a jacketed cylindrical 15-mL quartz cuvette attached to an optical train, which was equipped with an Osram XBO 150 W xenon arc lamp (I_0 (400−520 nm) = 2.0×10^{-6} Einstein s^{-1} cm^{-2}) installed in a light-condensing lamp housing (PTI, A1010S). When necessary, a cutoff filter was placed in front of the cuvette. Running water was circulated through the jacket to cool the reaction mixture, which was stirred magnetically.

In a typical experiment, 14 mL of a 0.5 g L^{-1} suspension of pure TiO_2 or Pt(IV)/AMM-Ti containing 4-CP, 2.5×10^{-4} mol L^{-1}, was sonicated for 15 min and then transferred to the cuvette. Before illumination, the suspension was magnetically stirred for 20 min to ensure complete phenol adsorption. During a run, ∼1.0 mL of the reaction solution was sampled at given time intervals. The sample was filtered through a Millipore membrane filter (0.22 μm pores) and then subjected to analysis by HPLC. For examining the photostability of Pt(IV)/AMM-Ti, a solution of the same composition as described above was first irradiated at $\lambda \geq 400$ nm for 6 h, which was long enough to degrade most of the 4-CP, as will be seen later; no sample was taken during the irradiation. Afterwards, the reaction solution was centrifuged to recover the catalyst, which was then washed two times with water. After drying in air at room temperature for 3 days, the catalyst was used again to repeat the photodegradation process, but this time, sampling was performed as described for the above suspension. Formation of CO_2 was detected gravimetrically by slowly bubbling O_2 through the reaction suspension (Pt(IV)/AMM-Ti, 0.5 g L^{-1}; 4-CP, 2.5×10^{-3} mol L^{-1}) and subsequently through a 10^{-2} M Ba^{2+} solution at pH 10−11. $BaCO_3$ was filtered off and dried at 60 °C for 3 days. The formation of HCl, another mineralized product from 4-CP, was confirmed by a quantitative measurement of the change in pH of the reaction solution. After almost complete disappearance of 4-CP, a pH value of 2.5−3.0 was obtained—nicely correlating with the stoichiometric decomposition.

HPLC (with a KromaSystem 2000 controller, a Kontron 320 autosampler, and a 430A photodiode array detector) was used to analyze 4-CP and aromatic intermediates in the samples. A reversed-phase C_{18} column (Kontron, Spherisorb 5 ODS 2) and water−methanol eluent (50:50) were employed. Absorbance at both 225 and 280 nm was used to determine the concentration of 4-CP and HQ.

Determination of Apparent Quantum Yields. Quantum yields were measured with an electronically integrating actinometer[25] to avoid errors related to fluctuations in the incident photon flux. The apparatus was calibrated with $Ru(bipy)_3^{2+}$.[26] In typical measurements, 3.0 mL of a 0.25 g L^1 suspension of Pt(IV)/AMM-Ti containing 2.5×10^{-5} mol of 4-CP per liter was sonicated for 15 min and subsequently transferred to the cuvette. At each wavelength, the reference cell contained a SiO_2 suspension having the same light-scattering properties as Pt(IV)/AMM-Ti at 800 nm. This procedure allowed an approximate measurement of the fraction of light absorbed by Pt(IV)/AMM-Ti, on the assumption that, as expected for large particles, the amount of scattered light was constant in the range of 335−800 nm. Both the sample cell and the reference cell were equipped with magnetic stirring to maintain a well-dispersed suspension. Using the main emission lines of the Osram HBO 500 W/2 medium-pressure Hg lamp, the irradiations were performed at 335, 366, 400, 436, and 546 nm. To investigate the intensity dependence of the quantum yield, we obtained variable photon fluxes by adjusting the width of the monochromator excitation slit. All measurements were carried out at a constant temperature of 25.0 °C. The calculation of the quantum yield was based on the disappearance of 4-CP as determined by HPLC.

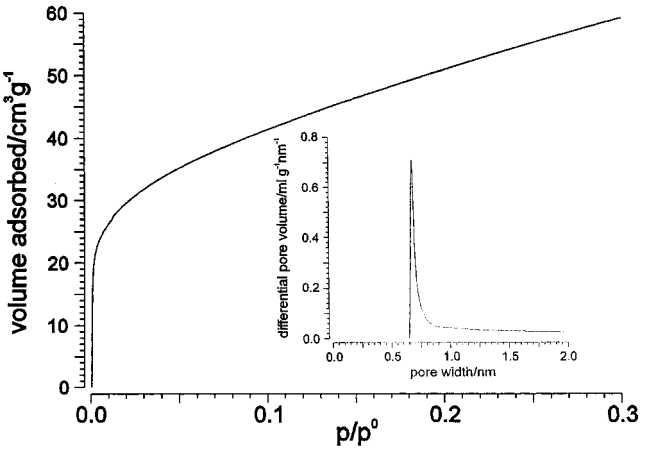

Figure 1. Ar adsorption isotherm of Pt(IV)/AMM-Ti. The insert shows the pore size distribution.

Results and Discussion

Characterization of Pt(IV)/AMM-Ti. The argon adsorption isotherm found is characteristic for a microporous material with a narrow pore-size distribution (Figure 1). Data treatment with the Horvath−Kawazoe method[21] revealed a maximum at 0.74 nm (insert in Figure 1). The material exhibited an unusually large surface area of 189 m^2/g, a property that may contribute to the good quantum efficiency in the photocatalytic applications.

Temperature-dependent XRD showed that the material is mainly amorphous phase. During the heating procedure, the anatase pattern starts to appear around 523 K. At 923 K, both anatase and rutile are present. At 1173 K, only rutile is detectable, but the amorphous phase is still dominantly present, as suggested by the low signal/noise ratio and the broad signal peak.

HRTEM examination of Pt(IV)/AMM-Ti samples indicated the presence of small crystalline regions (1−2 nm) embedded in the dominantly amorphous matrix (Figure 2). No order was detectable, suggesting a random orientation of the micropores. Despite the high contrast used, no distinct platinum particles could be observed, in agreement with the investigation by EDX, where platinum was detectable just barely above the noise level regardless of beam diameter and location. This implies that the doping platinum species are distributed homogeneously in the bulk matrix. The results of an EXAFS study at the platinum L_{III} absorption edge of Pt(IV)/AMM-Ti are presented in Figure 3. Both the experimental and the fitted $k^3\chi(k)$ functions and their corresponding Fourier transforms are shown. The $k^3\chi(k)$ function is typical for noncrystalline materials. There is no evidence for platinum in the first and second coordination shell, which is indicative of the absence of Pt clusters or Pt-chloride domains. For chlorine as backscatterer, the Pt−Cl distance,

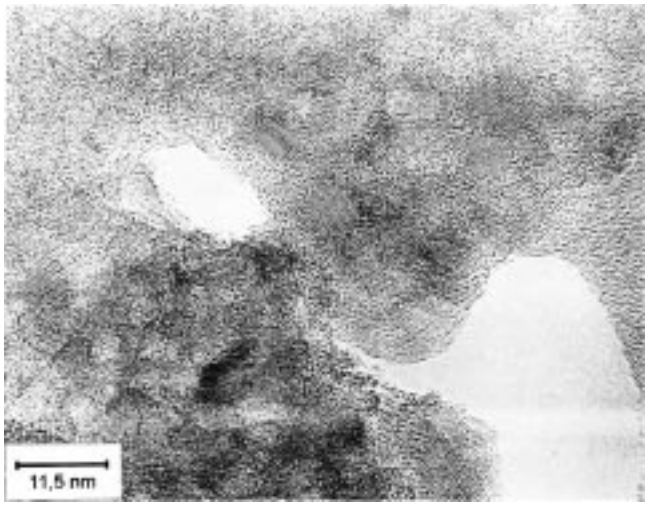

Figure 2. Representative TEM micrograph (×500,000) of Pt(IV)/AMM-Ti. Ordered spots show lattice fringes of small titania crystallites embedded in the amorphous TiO_2 matrix.

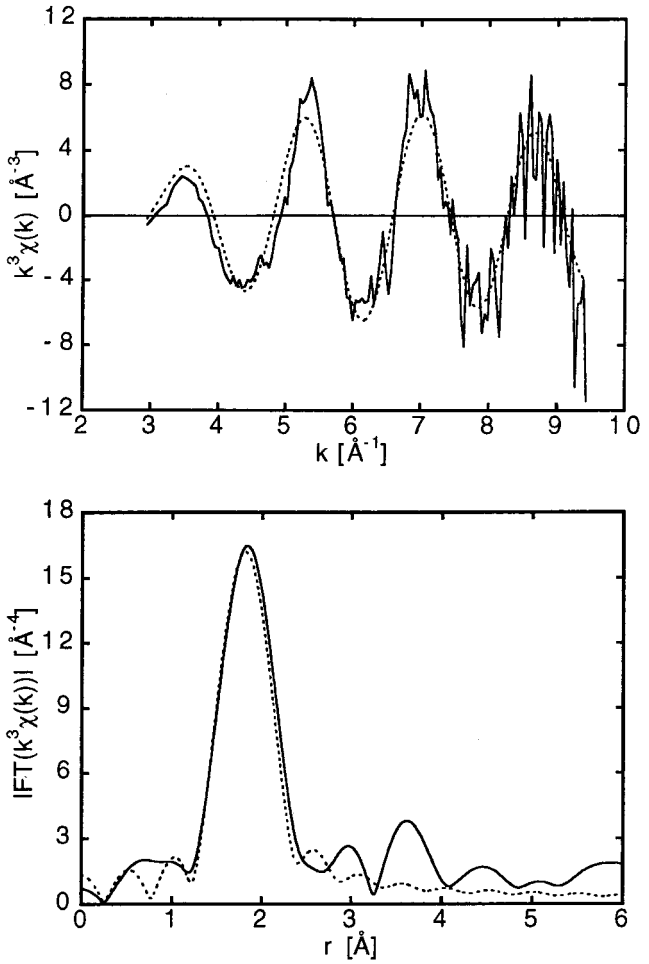

Figure 3. Experimental (solid) and calculated (dashed) $k^3\chi(k)$ functions above the platinum L_{III} absorption edge of Pt(IV)/AMM-Ti and the corresponding Fourier transform.

coordination number, and Debye−Waller factor are calculated as 2.28 Å, 4.3, and 0.079 Å, respectively.

Data analysis revealed that the main peak in the spectrum was entirely caused by chlorine backscatterers. Platinum backscatterers did not contribute significantly to the EXAFS spectrum. The oxidation number of the platinum atoms could not be determined from the EXAFS spectra, but as seen in Table 1 the Pt−Cl distance of 2.28 Å in the catalyst agrees best with the distance of 2.26 Å for $PtCl_4$. First X-ray photoelectron spectroscopy data showed a peak maximum at 74 eV, confirming the EXAFS assignment of Pt(IV) as the major platinum species.

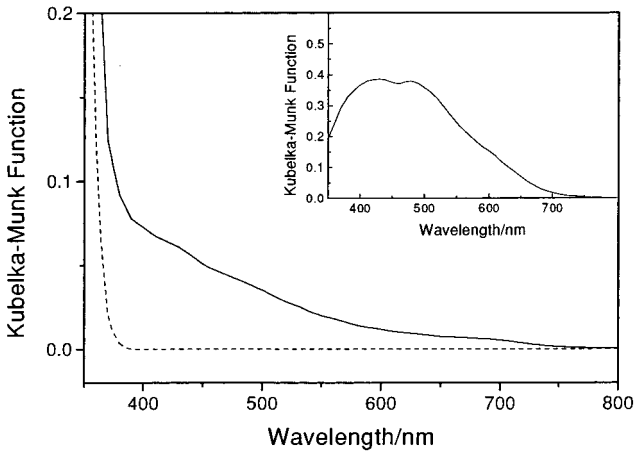

Figure 4. Diffuse reflectance spectra of P-25 TiO_2 (dotted curve), Pt(IV)/AMM-Ti (solid curve), and $PtCl_4$ (insert). Kubelka−Munk function, $F(R_\infty) = (1 - R_\infty)^2/2R_\infty$, is used as the equivalent of absorbance.

TABLE 1: Pt−Cl Distances in Crystalline Platinum Chlorides[31]

source	platinum chloride	Pt−Cl distance (Å)
Brodersen et al.[27]	β−$PtCl_2$	2.39−2.42
Falqui and Rollier[28]	$PtCl_2$(III)	2.32
Wiese et al.[29]	$PtCl_3$	2.31−2.45, 2.78
Falqui[30]	$PtCl_4$	2.26

The diffuse reflectance spectrum of Pt(IV)/AMM-Ti is shown in Figure 4, where the spectrum of commercial TiO_2 (P-25, Degussa) is also presented for comparison. Throughout the visible region, the new material exhibited significant absorption, in agreement with the brown-yellow color of the powder. Tentatively, we have assigned this absorption to the ligand field transition of the $PtCl_4$ modifier by analogy with solution spectra of corresponding chloro-complexes.[32] Solid $PtCl_4$ itself has a similar reflectance spectrum (insert in Figure 4). At short wavelengths below 400 nm, the absorption of Pt(IV)/AMM-Ti increased sharply, indicating band gap absorption of AMM-Ti, as inferred from the absorption feature of P-25 TiO_2.

Photodegradation of 4-CP. Upon irradiation of Pt(IV)/AMM-Ti with UV light ($\lambda \geq 335$ nm), photodegradation of 4-CP occurred in the presence of air, as shown in Figure 5. Under identical conditions the unmodified AMM-Ti exhibited only a very weak activity. This differs significantly from crystalline TiO_2, which is an efficient photocatalyst when illuminated with UV light.[33−35] The very poor activity of AMM-Ti most likely is due to the traces of crystalline TiO_2 observable by HRTEM. This is in accord with a recent finding of Ohtani et al. that amorphous TiO_2 does not photocatalyze the dehydrogenation of 2-propanol.[36] They attributed this finding to the abundant defects on the surface and in the bulk, all of which promote efficient recombination of photogenerated charge carriers.

Surprisingly, Pt(IV)/AMM-Ti catalyzed photodegradation even upon visible-light irradiation ($\lambda \geq 400$ nm). The activity was comparable with that in the UV region. For example, the initial rates at $\lambda \geq 335$ nm and $\lambda \geq 400$ nm were 2.8×10^{-4} mol L^{-1} h^{-1} and 1.2×10^{-4} mol L^{-1} h^{-1} respectively. For comparison, AMM-Ti and P-25 TiO_2 induced only an almost negligible reaction and no intermediates were detected, whereas

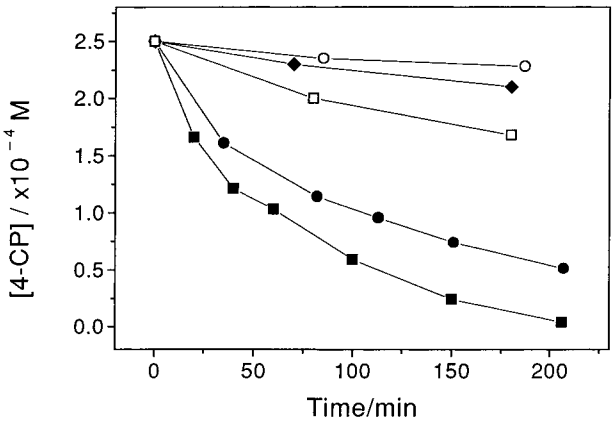

Figure 5. Photodegradation of 4-CP upon irradiating Pt(IV)/AMM-Ti with UV (■, $\lambda \geq 335$ nm) or visible light (●, $\lambda \geq 400$ nm). For comparison the reactivity of P-25 TiO_2 under visible illumination (◆, $\lambda \geq 400$ nm), and AMM-Ti under UV (□, $\lambda \geq 335$ nm) and visible (○, $\lambda \geq 400$ nm) irradiation, are also presented.

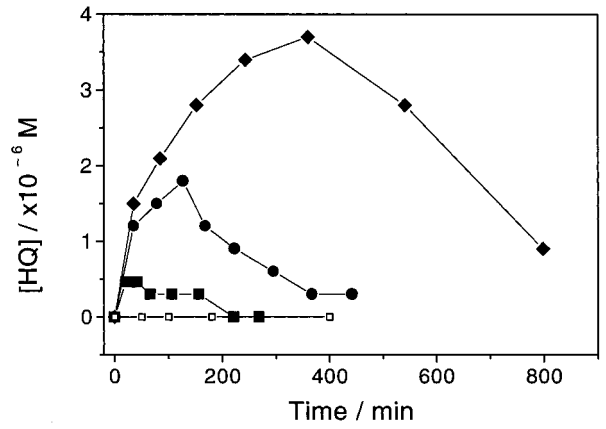

Figure 6. Changes in the concentration of hydroquinone (HQ) during the photodegradation of 4-CP in the suspension of Pt(IV)/AMM-Ti upon illumination in various wavelength regions: (□) $\lambda \geq 335$ nm; (■) $\lambda \geq 375$ nm; (●) $\lambda \geq 455$ nm; (◆) $\lambda \geq 530$ nm.

the intermediate HQ was observable in the Pt(IV)/AMM-Ti photocatalysis. From these results we conclude that the activity of the new hybrid titania originates from light absorption by the $PtCl_4$ component. We have examined a series of Pt(IV)/AMM-Ti samples containing platinum from 0.7 to 4.0 wt %, and found an optimum value around 3.0%.[37]

Recently we observed that the production of intermediates in TiO_2-catalyzed photodegradations strongly depended on the irradiation intensity.[33] In this study, when we used different cutoff filters, the concomitant changes in illumination intensity resulted in different concentration vs time curves for the intermediate HQ (Figure 6). At $\lambda \geq 335$ nm, where light intensity is highest, no HQ could be detected because of its fast decomposition, whereas at $\lambda \geq 375$ nm HQ was formed in low amounts. With visible light ($\lambda \geq 455$ nm) the maximum in the concentration−time curve of HQ was increased and was displaced to longer illumination time. This behavior was more pronounced at $\lambda \geq 530$ nm. These observations indicate that with decreasing light intensity, intermediates can be accumulated; since we found no intrinsic difference for UV and visible light illumination, the photocatalytic mechanism is apparently similar in both spectral regions.

The stability of a semiconductor photocatalyst can be affected by several factors such as photocorrosion and poisoning by intermediates or products. Normally the latter can be eliminated by washing the catalyst, whereas the former may be fatal (i.e., the activity will be lost completely). We checked the catalytic activity of Pt(IV)/AMM-Ti under three different conditions. When used for the second time without washing, the activity decreased by 50%, whereas the photodegradation still proceeded steadily. Upon washing this catalyst with water for two times, the activity was recovered by 90%.

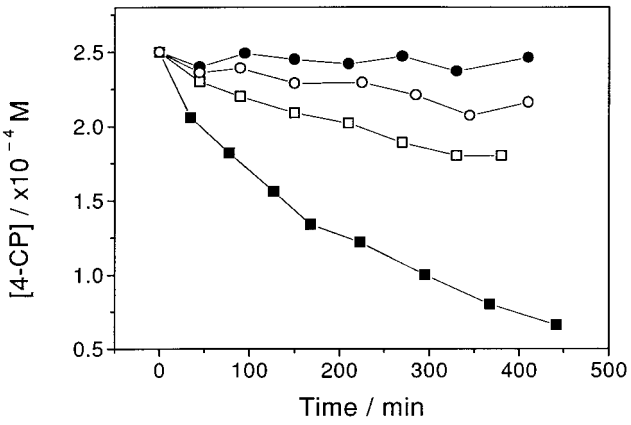

Figure 7. Comparison of photodegradation at $\lambda \geq 455$ nm of 4-CP by AMM-Ti modified with different platinum compounds: (■) 1.1% platinum(IV)chloride; (□) 1.0% platinum(IV)bromide; (○) 1.0% platinum(II)chloride; (●) 1.3% surface-loading of TiO_2 with PtO_2. The 1.3% PtO_2 bulk-doped TiO_2 exhibited the same negligible reactivity.

Comparative Investigations. The photocatalytic behavior of Pt(IV)/AMM-Ti may be caused by a metal−metal (MM) transition between Pt(IV) and Ti(IV), just as proposed for the Cr(III)-doped TiO_2.[9] However, that this is very unlikely is suggested by the photoactivity of an AMM-Ti sample modified with $PtBr_4$, which has the same crystal structure as $PtCl_4$ and similar chemical properties. One would expect the photodegradation of 4-CP by the former to proceed with a rate similar to that by Pt(IV)/AMM-Ti, if the Pt(IV)−Ti(IV) transition accounts for the photoactivity. However, the photodegradation by $PtBr_4$-modified TiO_2 under the same illumination conditions was much slower than that by $PtCl_4$ (Figure 7). This weaker activity will be discussed later. Figure 7 also shows that the platinum(II) chloride-modified TiO_2 is a very poor photocatalyst. This again disagrees with the possibility that the MM transition is involved; otherwise, the photoactivity of Pt(II)-modified TiO_2 should be higher than that of the Pt(IV)-modified sample because the Pt(II)−Ti(IV) transition is thermodynamically more feasible than Pt(IV)−Ti(IV).

We have also checked the photoactivity of amorphous titania mixed with PtO_2, given suspicions that traces of PtO_2 may form during the preparation and subsequent heating treatment of Pt(IV)/AMM-Ti. Two kinds of these mixed oxides were prepared and used as catalysts for the photodegradation of 4-CP, one prepared by bulk doping of amorphous TiO_2 with PtO_2 and the other by surface deposition of TiO_2 with PtO_2. As shown in Figure 7, the reaction was negligible in both cases, even though the TiO_2 and PtO_2 are believed to be in tight contact through the preparation procedure. This finding clearly excludes the possibility that PtO_2 is involved in the photocatalysis. Reduction of the Pt(IV)/AMM-Ti with hydrogen in the gas phase at 250 °C for several hours significantly decreased the photocatalytic activity and reduction for several days produced an inactive catalyst, indicating that the lower oxidation states of Pt are photocatalytically inactive.

Wavelength Dependence of Apparent Quantum Yield. As an important parameter of the activity of various photocatalysts, quantum yields were determined previously for TiO_2-photocatalyzed degradation of pollutants.[38−40] Because of problems

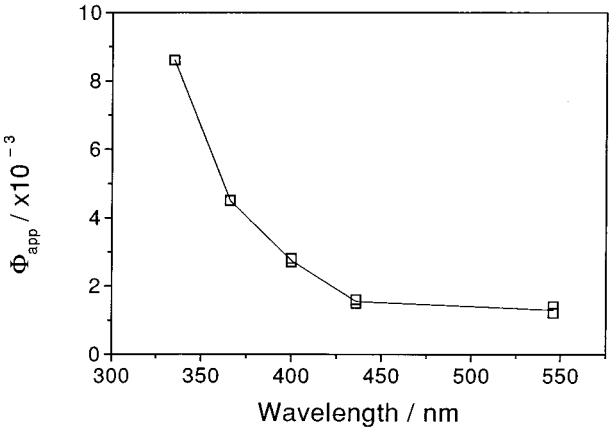

Figure 8. Apparent 4-CP disappearance quantum yields (Φ_{app}) in the suspension of Pt(IV)/AMM-Ti at various illumination wavelengths. See the text for the experimental details.

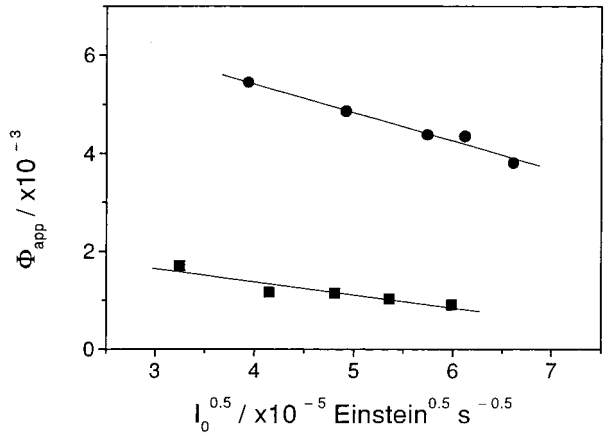

Figure 9. Photon flux (I_0) dependence of quantum yield (Φ_{app}) for excitation wavelengths 366 (●) and 436 (■) nm.

of light scattering, most of the reported quantum yields are apparent values, although Sun and Bolton[41], who used a modified integrating sphere method to measure the true fraction of light absorbed in the TiO_2 suspension, obtained a true quantum yield for the photochemical generation of OH radicals. In the present case, however, the dependence of apparent quantum yield (Φ_{app}) is sufficient to compare the activity of the new photocatalyst in the UV and visible spectral regions.

As evident from Figure 8 the apparent quantum yield changes only marginally in the visible region but increases sharply below 400 nm. This behavior parallels the wavelength dependence of the photoaquation quantum yield of $[PtCl_6]^{2-}$ in water solution, which is believed to occur through a platinum(III) intermediate.[32] We therefore assume that the photocatalytic activity of Pt(IV)/AMM-Ti is caused by photoexcitation in the platinum(IV) chloride part. Figure 8 also correlates well with the action spectrum of the photocurrent measurement carried out by loading Pt(IV)/AMM-Ti on a conductive glass electrode.[42]

Intensity Dependence of Quantum Yield. Figure 9 shows the relation of Φ_{app} with the incident photon flux at 366 and 436 nm excitations. In both cases the quantum yield is inversely proportional to the square root of the incident photon flux, which is consistent with the result obtained by Kormann et al.,[43] who investigated the photodegradation of chloroform by unmodified TiO_2 powder. Sun and Bolton[41] found a similar dependence for the true quantum yield of TiO_2-catalyzed photogeneration of OH radicals. Accordingly, at a higher photon flux, the resulting higher concentration of the charge carriers enhances

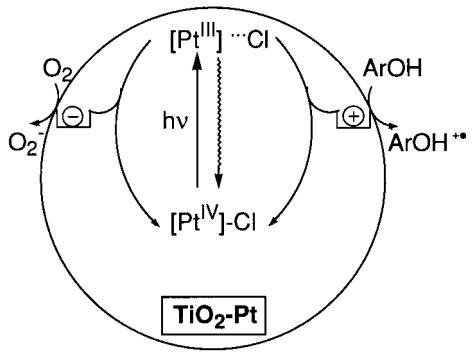

Figure 10. Pictorial view of the postulated primary processes occurring after light absorption by Pt(IV)/AMM-Ti.

recombination. As a result, the relative number of reactive charge carriers available for the interfacial redox reactions is decreased. The similar dependence of Φ_{app} on irradiation intensity in the UV and visible region suggests that the same mechanism operates in both spectral regions.

Mechanistic Proposal. Although the products and intermediates of 4-CP photodegradation correspond to the reaction catalyzed by crystalline TiO_2, the results presented above make it obvious that a completely different mechanism of charge generation must operate for the new amorphous photocatalysts. Recall that the photoactivity is bound to the presence of low amounts of a platinum(IV) halide homogeneously distributed over a large excess of amorphous microporous titania. By analogy then with the solution photochemistry of $PtCl_6^{2-}$,[44] we postulate as a working hypothesis the simple mechanism schematically depicted in Figure 10. Local excitation of the platinum halide in the UV or visible region affords charge-transfer-ligand-to-metal or ligand field states, respectively, which both undergo homolytic Pt-X bond cleavage to yield Pt(III) and a halogen atom, as observed also for homogeneous aqueous solutions.[32] The labile platinum(III) intermediate will rapidly transfer an electron to a Ti(IV) site of the amorphous TiO_2 matrix, while the chlorine atom abstracts an electron from the oxygen lattice. Both processes should be facilitated by the homogeneous distribution of platinum chloride within the metal oxide phase. At the resulting oxidizing and reducing surface centers, oxidation of the phenol and reduction of oxygen can occur, followed by complete mineralization, as known from the reaction photocatalyzed by crystalline TiO_2. Unlike in a homogeneous solution, however, the efficient back-reaction between the halogen atom and Pt(III) is partially suppressed by the surrounding TiO_2 matrix. In agreement with this hypothesis is the lower activity of the platinum(IV)bromide-modified AMM-Ti, since charge trapping by the less-oxidizing bromine atom may be less efficient.

This mechanism of photoinduced charge generation significantly differs from that of metal ion−doped crystalline TiO_2. In the latter case, light absorption occurs between states localized on both the doping metal ion and the semiconductor, whereas in the former, only the "doping" metal salt is involved. Since numerous other transition metal halides absorb in the visible region and can undergo photoinduced homolytic bond cleavage,[45−47] further work pursuing this route is in progress.

Conclusion

In summary, we found that an otherwise inactive amorphous, microporous titania powder upon modification with a few percent of platinum(IV)halide became a new type of inorganic hybrid photocatalyst for the visible light photodegradation of

4-CP. The results suggest that the dopant platinum halide initiates the reaction in both the UV and visible regions through homolytic cleavage of the platinum-halogen bond and subsequent charge-trapping by the amorphous titania matrix. From the reducing and oxidizing surface sites that result, the photodegradation occurs by analogy with the known mechanism of the UV photodegradation catalyzed by unmodified, crystalline titanium dioxide.

Acknowledgment. L.Z. thanks Alexander von Humboldt Foundation for a research fellowship. H.K. is indebted to B. Bogdanovic for stimulating discussions. This work was supported by Fonds der Chemischen Industrie.

References and Notes

(1) (a) Bard, A. J. *Science* **1980**, *207*, 139. (b) Heller, A. *Science* **1984**, *233*, 1141. (c) Grätzel, M. *Heterogeneous Photochemical Electron Transfer*, CRC Press: Boca Raton, FL, 1988. (d) Memming, R. *Top. Curr. Chem.* **1988**, *143*, 79. (e) Koval, C. A.; Howard, M. N. *Chem. Rev.* **1992**, *92*, 411.

(2) (a) Fox, M. A.; Dulay, M. T. *Chem. Rev.* **1993**, *93*, 341. (b) Kraeutler, B.; Bard, A. J. *J. Am. Chem. Soc*. **1978**, *100*, 2239. (c) Sakata, T.; Kawai, T.; Hashimoto, K. *J. Phys. Chem*. **1984**, *88*, 2344. (d) Ohtani, B.; Watanabe, T.; Honda, K. *J. Am. Chem. Soc.* **1986**, *108*, 308. (e) Wang, C. M.; Mallouk, T. E. *J. Am. Chem. Soc.* **1990**, *112*, 2016.

(3) (a) Schiavello, M., Ed. *Photocatalysis and Environment*; Kluwer Academic Publishers: Dordrecht, 1988. (b) Ollis, D. F.; Al-Ekabi, H., Eds. *Photocatalytic Purification and Treatment of Water and Air*; Elsevier: Amsterdam, 1993. (c) Legrini, O.; Oliveros, E.; Braun, A. M. *Chem. Rev.* **1993**, *93*, 671. (d) Lewis, L. N. *Chem. Rev.* **1993**, *93*, 2693. (e) Matthews, R. W. *Pure Appl. Chem*. **1992**, *64*, 1285.

(4) See for example: Kamat, P. V. *Chem. Rev*. **1993**, *93*, 267; and references therein.

(5) Lawless, D.; Kapoor, S.; Meisel, D. *J. Phys. Chem*. **1995**, *99*, 10329.

(6) Vogel, R.; Hoyer, P.; Weller, H. *J. Phys. Chem*. **1994**, *98*, 3183.

(7) Spanhel, L.; Weller, H.; Henglein, A. *J. Am. Chem. Soc*. **1987**, *109*, 6632.

(8) Gopidas, K. R.; Bohorquez, M.; Kamat, P. V. *J. Phys. Chem*. **1990**, *94*, 6436.

(9) Borgarello, E.; Kiwi, J.; Grätzel, M.; Pelizzetti, E.; Visca, M. *J. Am. Chem. Soc*. **1982**, *104*, 2996.

(10) Bahnemann, D. W.; Bockelmann, D.; Goslich, R.; Hilgendorff, M. In *Aquatic and Surface Photochemistry*; Helz, G. R.; Zepp, R. G.; Crosby, D. G., Eds.; Lewis Publishers: Boca Raton, FL, 1994; pp 349−367.

(11) Hoffmann, M. R.; Martin, S. T.; Choi, W.; Bahnemann, D. W. *Chem. Rev.* **1995**, *95*, 69.

(12) Keck, H.; Schindler, W.; Knoch, F.; Kisch, H. *Chem. Eur. J*. **1997**, *3*, 1638.

(13) Maier, W. F.; Bohnen, F. M.; Heilmann, J.; Klein, S.; Ko, H.-C.; Mark, M. F.; Thorimbert, S.; Tilgner, I.; Wiedorn, M. In *Applications of Organometallic Chemistry in the Preparation and Processing of Advanced Materials*; Harrod, J. F.; Laine, R. M., Eds.; NATO ASI−Series, Kluwer Academic Publishers: Dordrecht, 1995; pp 27−46.

(14) Klein, S.; Maier, W. F. *Angew. Chem*. **1996**, *108*, 2376; Int. Ed. **1996**, *35*, 2330.

(15) Klein, S.; Thorimbert, S.; Maier, W. F. *J. Catal*. **1996**, *163*, 477.

(16) Maier, W. F.; Klein, S.; Martens, J.; Heilmann, J.; Parton, R.; Vercuysse, K.; Jacobs, P. A. *Angew. Chem.* **1996**, *108*, 222; Int. Ed. **1996**, *35*, 180.

(17) Storck, S.; Maier, W. F.; Salvado, I. M. M.; Ferreira, J. M.; Guhl, D.; Martens, J. A.; Souverijns, W. *J. Catal.* **1997**, *172*, 414.

(18) Klein, S.; Martens, J.; Parton, R.; Vercuysse, K.; Jacobs, P. A.; Maier, W. F. *Catal. Lett.* **1996**, *38*, 209.

(19) Lange, C.; Tesche, B.; Storck, S.; Maier, W. F. *J. Catal*. **1998**, *175*, 280.

(20) Maier, W. F.; Ko, H. C. *Catal. Today* **1995**, *25*, 429.

(21) Horvath, G.; Kawazoe, K. *J. Chem. Eng. Jpn.* **1983**, *16*, 470.

(22) Kortum, G. *Reflectance Spectroscopy*; Springer-Verlag: New York, 1969.

(23) Ertel, T. S.; Bertagnolli, H.; Hückmann, S.; Kolb, U.; Peter, D. *Appl. Spectrosc.* **1992**, *46*, 690.

(24) Mustre de Leon, J.; Rehr, J. J.; Zabinsky S. I.; Albers, R. C. *Phys. Rev. B* **1991**, *44*, 4146.

(25) Amrein, J.; Gloor, J.; Schaffner, K. *Chimia* **1974**, *29*, 185.

(26) Görner, H.; Kuhn, H. J.; Schulte-Frohlinde, D. *EPA Newsl.* **1987**, No. 31, 13.

(27) Brodersen, K.; Thiele, G.; Schnering, H. G. v. *Z. Anorg. Allg. Chem.* **1965**, *337*, 120.

(28) Falqui, M. T.; Rollier, M. A. *Ann. Chim. Roma* **1958**, *48*, 1154.

(29) Wiese, U.; Schäfer, H.; Schnering, H. G. v.; Brendel, C.; Rinke, K. *Angew. Chem.* **1970**, *82*, 135.

(30) Falqui, M. T. *Ann. Chim. Roma* **1958**, *48*, 1160.

(31) The Pt−Cl distances are calculated with the program ATOMS 2.44a (Ravel, B. University of Washington, Department of Physics) from the crystal parameters given in the references.

(32) Cox, L. E.; Peters, D. G.; Wehry, E. L. *J. Inorg. Nucl. Chem.* **1972**, *34*, 297.

(33) Zang, L.; Liu, C.-Y.; Ren, X.-M. *J. Chem. Soc., Faraday Trans*. **1995**, *91*, 917.

(34) Al-Ekabi, H.; Serpone, N.; Pelizzetti, E.; Minero, C.; Fox, M. A.; Draper, R. B. *Langmuir* **1989**, *5*, 250.

(35) Matthews, R. W. *J. Catal*. **1988**, *111*, 264.

(36) Ohtani, B.; Ogawa, Y.; Nishimoto, S. *J. Phys. Chem.* **1997**, *101*, 3746.

(37) Detailed information to be published elsewhere.

(38) Lepore, G. P.; Langford, C. H.; Vichova, J.; Vleck, A. Jr. *J. Photochem. Photobiol. A: Chem*. **1993**, *75*, 67.

(39) Matthews, R. W.; McEvoy, S. R. *J. Photochem. Photobiol. A: Chem*. **1992**, *64*, 93.

(40) Anpo, M.; Shima, T.; Kodama, S.; Kubokawa, Y. *J. Phys. Chem*. **1987**, *91*, 4305.

(41) Sun, L.; Bolton, J. R. *J. Phys. Chem*. **1996**, *100*, 4127.

(42) Kisch, H.; Zang, L.; Lange, C.; Maier, W. F.; Antonius, C.; Meissner, D. *Angew. Chem., Int. Ed. Engl.* **1998**, *37*, 3034.

(43) Kormann, C.; Bahnemann, D. W.; Hoffmann, M. R. *Environ. Sci. Technol*. **1991**, *25*, 494.

(44) Ford, P. C.; Wink, D.; DiBenedetto, J. *Prog. Inorg. Chem.* **1983**, *30*, 213.

(45) Horvath, O.; Stevenson, K. L. *Charge-Transfer Photochemistry of Coordination Compounds*; VCH Publishers: New York, 1993.

(46) Kartuzhanskii, A. L.; Plachenov, B. T.; Studzinskii, O. P. *Izv. Vyssh. Uchebn. Zaved. Khim., Khim. Tekhnol*. **1990**, *33*, 3.

(47) Moggi, L.; Varani, G.; Manfrin, M. F.; Balzani, V. *Inorg. Chim. Acta* **1970**, *4*, 335.